American Journal of Engineering Research (AJER) 2015
American Journal of Engineering Research (AJER)
e-ISSN: 2320-0847 p-ISSN : 2320-0936
Volume-4, Issue-9, pp-160-167
www.ajer.org
Research Paper Open Access

Fluid Flow through Woven Fabrics by the Lattice-Boltzmann Method

[1]Mohammad Miyan, [2]Pramod Kumar Pant
[1]*Department of Mathematics, Shia P. G. College, University of Lucknow, Lucknow, India*
[2]*Department of Mathematics, Bhagwant University, Ajmer, Rajasthan, India*

ABSTRACT: *The Lattice- Boltzmann method is used for investigating the dual scale problems of the fluid flow through three dimensional multifilament woven fabrics. These fabrics are generally characterized by two different length scales i.e., the thickness of a single filament and the thickness of a bundle of filaments, known as yarn. The thickness of yarn is of the two orders of magnitude greater than that of the single filament. The inter-yarn and intra-yarn spaces are also of the two different scales. The direct simulation of fluid flow in multifilament woven fabrics includes the resolution of the flow in the inter-yarn and intra-yarn pores of the media.In the present paper, there is an analysis of the fluid flow in woven fabrics with the Lattice-Boltzmann method. The tortuosities are given by the LB simulations and image analysis. The transverse and in plane tortuosities were determined by LB flow simulations and by image analysis that uses the chord length distribution algorithm [20]. The paper sheets formed as strictly layered structures in the laboratory sheet mold show little change in tortuosity with changing porosity as the fibres were refined the density of the sheet was increased. Hence, the transverse tortuosity has a significant change as a result of refining and densification. That indicates a more complex and less permeable structure. The chord length method tends to give higher values for tortuosity since the hydrodynamic tortuosity given by the LB method gives more weight to paths of least resistance, whereas this method does not prefer any particular fluid path or chord length. The graphs show that the toruosity varies inversely with porosity of the media. The results are shown with the help of tables and figures.*

Keywords: *Flow, Woven Fabrics, Porous Media, Lattice-Boltzmann method.*

I. INTRODUCTION

The woven fibrous porous media can be found in various industrial applications including but unlimited to preforming in polymer liquid composite mouldings, filters for separation of solid particles and the gas diffusion layer of proton exchange membrane fuel cells. The application that is of main interest in the present paper is the flow in the woven fabrics preform of the resin transfer moulding (RTM) process. The RTM process is a popular method for manufacturing of both the small and large composite parts. The main challenge in the RTM process is the prediction of resin flow in the mould through perform. So the knowledge of the resin flow pattern inside the mould is necessary for the determination of optimum location of the air vents and injection gates on the mould for reducing the possibility of void formation in the manufactured parts. The preform is usually in the form of multifilament yarns bound together in the different forms and structures. In this work, we focus on preforms constructed from woven fabrics;

Hu [10] and Chou [5] have discussed the design and properties of the micro structure of woven perform. Woven fabrics are generally characterized by two different length scales:

(a) The length scale of a single filament, (e.g. its radius)

(b) The length scale of a bundle of filaments (a yarn), which is usually about two orders of magnitude greater than that of a single filament.

Nabovati A. *et al.*, [14] have analyzed in details about the three-dimensional multifilament of woven fabrics. The woven fabrics have a dual porosity characteristic. The first defined porosity is related with the internal structure of a yarn, and is termed here the *yarn porosity* or *y*. The yarn porosity gives the voids between the constituent filaments of a yarn and characterizes the intra-yarn flow. This is defined as the ratio of the void volume within a yarn to the total volume of the yarn. The second porosity is due to the void spaces between the yarns and is termed as the *weave porosity* or *w*. So, for calculating the weave porosity, the yarns are taken as a

solid *i.e.*, zero yarn porosity; so the weave porosity is taken as the ratio of the void volume between the yarns to the total volume of the minimal bounding box of the fabric sheet. The simulations of fluid flow through woven porous media capture the flow through both the yarn and weave porosities. The easiest structural form of fibrous media that has been studied in the analysis is a regular array of infinitely long solid cylinders. Sangani *et al.* [22], Gebart [6], and Bruschke *et al.* [4] studied the flow around solid cylinders of infinite length with square and hexagonal arrangements and proposed correlations for the axial and transverse flow permeabilities. The flow in solid yarn woven fabrics was first characterized by using the orifice analogy [4], [19], in which the pores between the yarns were considered as a series of orifices and the discharge coefficient was given as a function of the pore structure. Later Lu *et al.* [12] investigated numerically the fluid flow in a monofilament filter cloth by using the commercial software, employing the finite volume method to simulate fluid flow in three basic, bi-axial, plain-weave models for the woven filters. Based on these three weave-models, four different pore structures were extracted to use in the fluid flow simulations. The corrected form for the discharge coefficient in the orifice model was proposed based on the simulation results. With the orifice analogy, Gooijer *et al.* [8] developed a geometrical model for the flow resistance
in monofilament woven fabrics by using the four unit pore structures of Lu *et al.* [12]. The proposed structure was in good agreement with the experimental data. With the methodology of Lu *et al.* [12] and Wang *et al.* [23] simulated fluid flow in a unit cell of monofilament woven fabric and given the values related to the discharge coefficient for fabrics with elliptical cross sections. By which, they found that the discharge coefficient decreases with the increasing aspect ratio of the cross-section of the fibres. Simulating fluid flow in multifilament woven samples is a hard and challenging task due to the dual scale nature of the weave and yarn structures. But the directly simulating flow at both scales is computationally expensive. So one popular approach is to simulate the fluid flow in two dimensions in the place of three dimensions. These simulations are less demanding and they are not able to predict the effects of the curvature of yarns and their relative structure on the overall permeability of the multifilament woven samples. Papathanasiou [15] solved numerically the Stokes equation in two dimensions by using the Boundary Element Method in square arrays of permeable multifilament yarns, in which every yarn was made up of circles representing the cross sections of the constituent filaments. So the effective permeability of the medium was found as a function of the weave and yarn porosities. In the same patterns the studies were performed for the square and hexagonal arrangement of filaments in yarns, where the yarns had the circular cross section [13] and for yarns with elliptical cross section [16]. Papathanasiou [17] had given a correlation for the effective permeability of two-dimensional hexagonal arrangements of filament clusters as a function of the weave and yarn permeabilities given by the formula:

$$K_p = K_w \left\{ 1 + \alpha \left(\frac{K_w}{K_y} \right)^{n-\frac{3}{2}} \right\} \tag{1}$$

Where K_p is the effective permeability of the multifilament fabric, K_w is the weave permeability, K_y is the permeability of the cross-sections of yarns and α and n are constants related to the geometric structure of the fabric. The given relationship is based on dimensional arguments and from consideration of the behavior at high and low *Kw/Ky* ratio asymptotes. Papathanasiou [17] had given values for α and n by fitting to the numerical simulation data and obtained the values as follows:
(1.1) $\alpha = 2.3$ and $n = 0.59$; when filaments are arranged in a square array,
(1.2) $\alpha = 3.0$ and $n = 0.625$; when filaments are arranged in a hexagonal array.
The author claims that values of $\alpha = 2.67$ and $n = 0.61$ give an acceptable fit for both square and hexagonal ordered
structures of filaments in the clusters and for high yarn and low weave porosities. For a two dimensional case, the K_w and K_y depend on the weave and yarn porosities, so the arrangement of the filaments inside the yarns and the arrangement of the yarns themselves. The flow in an ordered structures of cylinders has been studied in depth and
various correlations for the transverse permeability, K, of the media have been given, in which the taken relationship is given by Gebart [6] is one of the mostly used *i.e.*,

$$\frac{K}{R^2} = C \left\{ \sqrt{\frac{1-\phi_c}{1-\phi}} - 1 \right\}^{\frac{5}{2}} \tag{2}$$

Where R is the radius of the cylinder, ϕ is the porosity of the medium, ϕ_c is the critical value of porosity below which the fibres make contact and there is no permeating flow and C is a geometric factor which depends on the type of the packing;
Gebart calculates the values as follows:
(1.3) $C=16/9\pi\sqrt{2}$, $\phi_c=1-\pi/4$ for the square array of cylinders,

(1.4) $C=16/9\pi\sqrt{6}$, $\phi_c=1-\pi/2$ for the hexagonal array.

The equation (2) will be used for predicting K_y by setting R equal to the filament radius and ϕ equal to the yarn porosity and K_w can be predicted by setting R equal to the yarn radius and ϕ equal to the weave porosity. The polymeric carrier fabrics are generally used in industrial processes mostly including manufacture of paper and board. The 3D structures of the fabrics play a critical role for deciding the energy and manufacturing efficiency of the process and end-use properties of the product. Now the analysis is based by using X-ray μCT to visualize the 3D structure of polymeric fabrics commonly used in paper manufacturing. The 3D structural characteristics and fluid transport properties for the tomographic images were measured with the image analysis techniques and the Lattice-Boltzmann method.

II. TOMOGRAPHIC IMAGES

The X-ray tomographic images were taken by two different types of paper machine forming fabrics. The two samples of each wire type were imaged. The resolution of the images was 4.41 μm and 4.34 μm for the type I and type II samples respectively. A typical yarn diameter was thus of the order of 40 pixels, so the resolution of the images was very good, as for the level of discreteness effects. The lateral sizes of the rectangular images were about one unit cell of the wires that were about 2.3 × 2.2 mm^2 and 3.0 × 2.6 mm^2 for type- I and type-II wires respectively. The samples images of type-I and type-II of wires are given by figures-1 and figure-2 respectively.

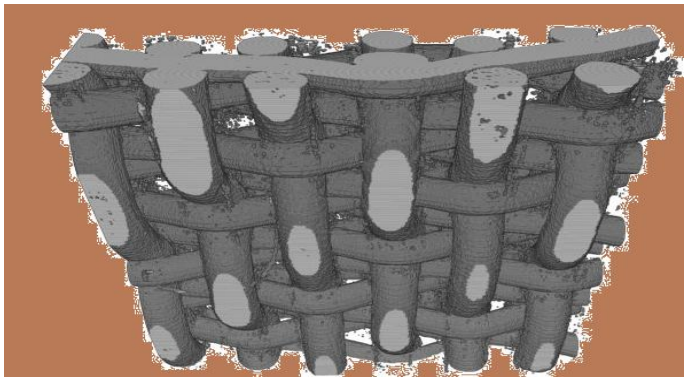

Figure-1 (Sample of the paper of type I)

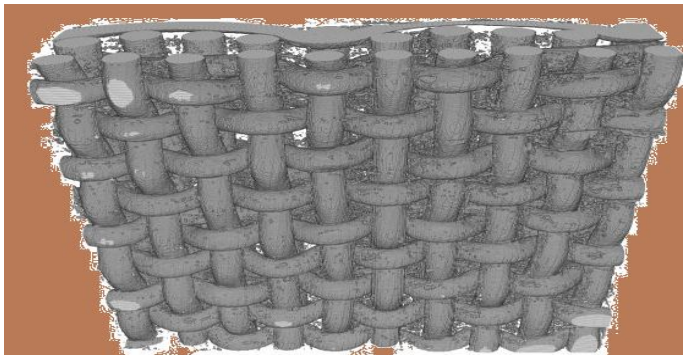

Figure-2 (Sample of the paper of type II)

The unlike disordered materials *i.e.*, paper, wires can be used to some extent to analyses the quality of the used tomographic images, as one can expect to obtain a regular interior structure. In this regard, one finds from the images that the surface of the wires seems rough and spurious tiny solid obstacles seem to be created by the imaging procedure within the pore space. In the similar manner, the solid phase seems to contain incidental small voids. So that the error created by the small irregularities can be analyzed to be very small *i.e.*, likely of the order of a few per cent.

Aaltosalmi U. analyzed in his thesis by taking the three different sample papers *i.e.*, filter paper, newsprint and hand sheets were taken to check the applicability of $X-\mu CT$ techniques. The hand sheet was made of bleached softwood Kraft pulp of spruce. The newsprint was made of thermo-mechanical pulp of spruce in a paper machine and the paper was not calendared. The filter paper was a circular black ribbon filter paper made of cotton linters. The Table -1 shows the thickness, density and basis weight of the imaged sample papers. The accuracies of these quantities are typically of the order of a few per cent, so the taken samples have the distinct characteristics and properties, so are expected to give distinct results in the image analysis and fluid transport simulations [1].

Table -1 (Bulk properties of the imaged sample papers)

Sample papers	*Thickness (µm)*	*Density (kg/m^3)*	*Basis weight (g/m^2)*
Hand sheet paper	98	647	63.4
Newsprint	109	403	44.1
Filter paper	158	486	76.7

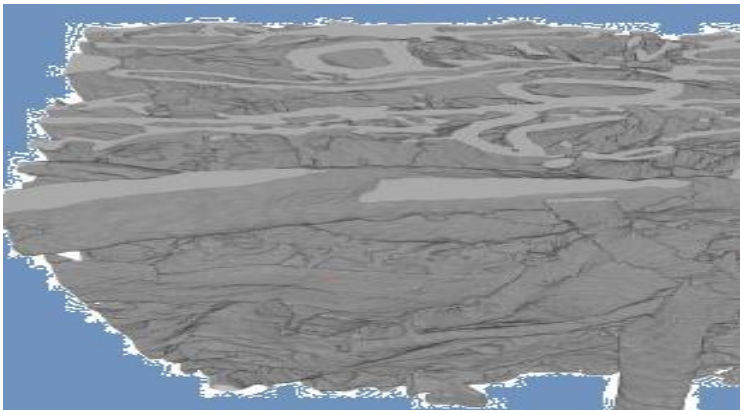

Figure-3(High resolution image of paper)

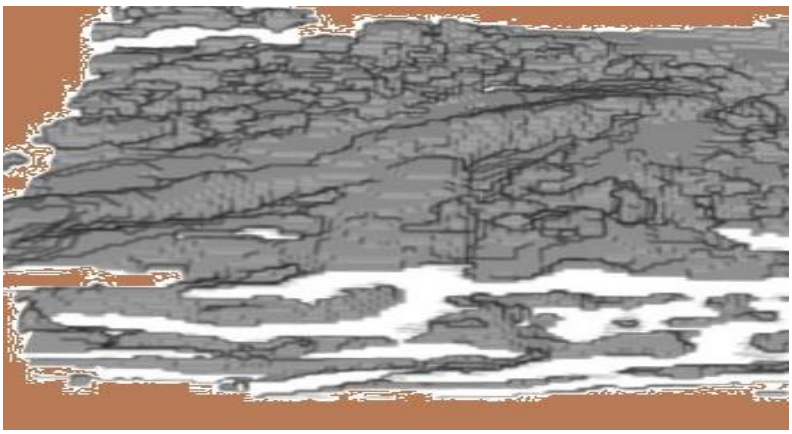

Figure-4(Low resolution image of paper)

So, to identify the necessary level of structural details for a reliable characterization of different paper grades, Aaltosalmi U. [1] used the samples imaged by using high and low resolution $X-\mu CT$ techniques. The figure-3 and figure-4 show high and low resolution images of newsprint paper. The relatively small image sizes *i.e.*, below 0.1 mm^2, were used in the high resolution and several low resolution images. Also a set with a larger image size *i.e.*, about 1 mm^2, was taken for the low resolution technique. The low resolution images were obtained using polychromatic radiation [11] and the high resolution images were obtained using monochromatic synchrotron radiation in the phase-contrast mode [21]. The low and high resolution images were reconstructed and processed according to the routines [2], [11]. The small detached volumes of fibrous and porous phases were removed by the 3-D filtering technique and the surfaces of the samples were defined using the rolling ball algorithm [3], [22]. Due to this algorithm surface is defined by the route of a ball with a suitable radius that rolls along the surface. This method allows the detection of the main structures of uneven surfaces excluding the interior pores [1].

The image analysis techniques [11], [20] were used to determine 3-D structural characteristics such as porosity, specific surface area, hydraulic pore-radius distribution and diffusive tortuosity in the principal directions. The diffusive tortuosity measurements were based on various successful paths of a random walk simulation through the paper volume with a random starting point on an appropriate volume edge [1].

Table-2 (Some properties founded from the *3-D* images of the samples)

Sample papers	Image size	Resolutions	Thickness T (μm)	Density ρ (kg/m^3)	Basis weight B_w (g/m^2)	Porosity ϕ (%)	Specific surface area $SSA(\times 10^3/m)$
Hand sheet paper	Small	High	90.1	829	74.9	46.4	303
	Small	Low	88.5	857	75.5	44.9	179
	Large	Low	101.5	796	79.6	49.0	176
News paper	Small	High	99.3	655	65.1	57.7	387
	Small	Low	119.2	651	76.1	58.2	179
	Large	Low	115.7	655	74.3	58.0	181
Filter paper	Small	High	190.9	550	105.5	64.3	234
	Small	Low	181.6	641	116.2	58.7	164
	Large	Low	179.4	570	101.8	63.4	157

The values were determined in the principal directions by Aaltosalmi U. [1]. So, such flow related objects parameters as the tortuosity of the flow paths and the permeability of flow in the transverse direction, were calculated by using direct numerical simulations with the Lattice-Boltzmann method. There is a use of a specific *LBGK* model with a uniform external body force and the bounce back boundary condition at the solid fluid interfaces. So, to ensure an unrestricted fluid flow at the inlet and outlet, a free fluid layer with the thickness of about 1/10 of the sample thickness was added on top of the sample and the boundary conditions were imposed in all outer boundaries of the rectangular computation volume. Then to compare the ability of the techniques of imaging to find out the correct amount of material in the imaged volumes, the quantities of table-1 *i.e.*, thickness, density and basis weight, were also computed by image analysis. The results shown in the table-2 are together with porosity and specific surface area. So, in the following, the values of low resolution samples are mean values obtained for available samples. The slight differences between the bulk properties and the image analysis results obtained in part from normal variation *i.e.*, are related to the formation of the samples used but also from the difference between the standard thickness and the rolling ball defined thickness and from a probable over estimation of the density of fibres *i.e.*, used in table-2 for all the papers. Hence the used techniques may over estimate the volume of the solid objects in the images. The specific surface area for the low resolution images is consistently less than that of the high resolution images. Now the observed differences are most probably occurs due to the differences in the level of detail. Then, it is clear from visual comparisons that the high resolution technique preserves the topology of the fibrous and porous structure objects better than the low resolution technique. But the large volume images are multiple times larger than the small volume images; there is no signified difference between the respective properties and characteristics. This indicates that even small volumes are sufficient and suitable for a good estimation of porosity and specific surface area.

III. TORTUOSITY AND PERMEABILITY

For a better understanding and analysis of the transport resistance of the samples, their tortuosities and permeabilities were measured by Aaltosalmi U. [1], and the results are shown by the table-3.

Table-3 (Tortuosity and permeability determined for various paper samples and imaging techniques)

Sample papers	Image size	Resolutions	τ_1	τ_2	τ_3	τ_4	ϕ
Hand sheet paper	Small	High	2.69	3.47	16.0	3.78	0.0363
	Small	Low	1.21	1.36	2.93	1.98	0.343
	Large	Low	1.25	1.36	3.25	2.11	0.325
News paper	Small	High	1.43	3.50	6.76	2.32	0.117
	Small	Low	1.12	1.56	3.57	2.04	0.524
	Large	Low	1.07	1.36	2.96	2.24	0.548
Filter paper	Small	High	1.23	1.33	4.69	1.58	1.95
	Small	Low	1.16	1.23	1.99	1.52	1.62
	Large	Low	1.10	1.17	1.61	1.55	2.78

In the table-3, τ_1, τ_2 and τ_3 are the diffusive tortuosity values in the machine direction, cross direction and transverse directions respectively obtained from the random walk simulations. τ_4 and ϕ are the flow tortuosity and permeability in the transverse direction obtained by using direct numerical simulation by the Lattice-Boltzmann method.

The largest differences between the tortuosities, in different sample papers as well as in the different principal directions, were observed in the high resolution images, due to their higher level of detail. The smallest differences were found in the small, low resolution images. Increase in the resolution will though increase the differences in the measured tortuosity and will thus improve the possibility to measure the effects of paper structure on the tortuosity and other transport properties and characteristics. The low resolution images will mainly provide right trends in these properties, so are useful for comparative studies. Their applicability is limited by their lower ability to analyze small particles such as fines, fillers and fibrils, and fibre-orientation anisotropy. The flow tortuosity τ_4 was found to be systematically lower than the diffusive transverse tortuosity τ_3.There are expectations since the streamlined hydrodynamic paths through the pore space are smoother than the winding random walk paths of diffusive particles. So that the dependence of the flow tortuosity on different structural properties of the samples is qualitatively similar to that of the diffusive tortuosity and the same qualitative analysis is suitable for both. About the results for permeability and flow tortuosity, there is no significant difference between the values calculated for small and large samples. Hence the permeabilities of the low resolution images are higher than those of the high resolution images. The difference is moderate at high porosities and becomes significant at lower porosities. Now, the poor resolution of the low resolution images makes dense, complex structures more open for transport, whereas already open and relatively simple structures are affected lesser. Particularly, the high resolution results seem to be in qualitative agreement with the known limiting behavior of flow tortuosity. This should approach unity as the porosity approaches unity and diverge at some small but non zero value of porosity. Generally, the results obtained for the high resolution samples by Aaltosalmi U. [1] will be taken more reliable and suitable. But the results discussed here, are qualitatively quite, they are subject to uncertainty arising from the limited available data and calculations. So to estimate the order of magnitude of purely numerical errors arising from the different used discretizations, there are a set of test samples by reducing the resolution of the original high resolution images to that of the low resolution images. The greatest difference between the tortuosities and permeabilities obtained for the original high resolution samples and the reduced resolution samples was about 1/5. The error due to the resolution could be compared with that due to sample size. The later was determined by dividing the original large images to several sub-images, the size of that coincided with that of the original smaller tomographic images. The greatest difference between the values calculated for the original large image and the mean value of the corresponding sub-images was about 1/20 for tortuosity and 1/5 for permeability and these values are very nearer with the values obtained by using *Kozeny's* law. The conclusion is that numerical uncertainties are not much suitable for the qualitative results obtained here. Instead, the natural variation intrinsic to paper material can be a much more important source of uncertainty for the results obtained on tomographic images. So, the uncertainties in the results are from the formation effect, to be of the order of a second factor in permeability and in the tortuosity.

IV. NUMERICAL SIMULATIONS

Aaltosalmi U. [1] analyses the numerical results of fluid flow through tomographic images of paper. The hand sheets of a basis weight of 300 g/m^2 were prepared from bleached softwood Kraft pulp, which was beaten to different refining levels between 220 and 670 *CSF* in a laboratory beater. The three dimensional $X-\mu CT$ images of the samples were made by using the phase contrast method [7], [9]. The resolution and the size of the images were about 2 μm and 1 mm^2 respectively. The paper surface layers were removed in the direction of the transverse axis, now the thicknesses of the final samples lie between 120 μm and 200 μm. The examples of structures observed by tomographic imaging of the paper samples are given by the figure-5. The images of these samples were observed for the transverse and inplane permeability, porosity, specific surface area, and tortuosity by using image analysis techniques [7], [20] and Lattice-Boltzmann flow simulations in the two orthogonal directions. So a reasonable comparison with conventional mercury intrusion porosimetry data from the same samples was obtained [20].

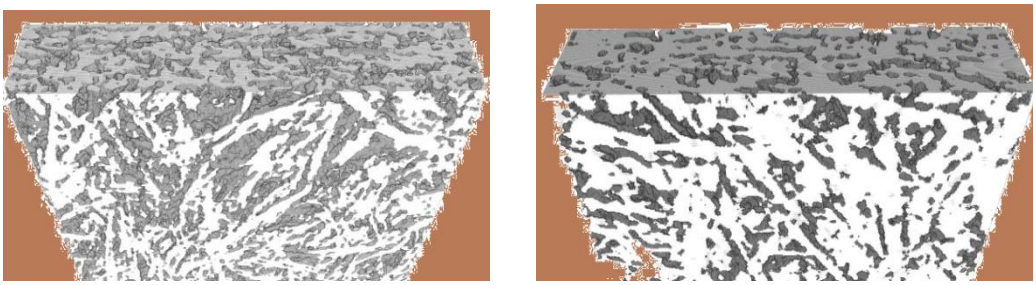

Figure-5 (Tomographic images of paper samples)

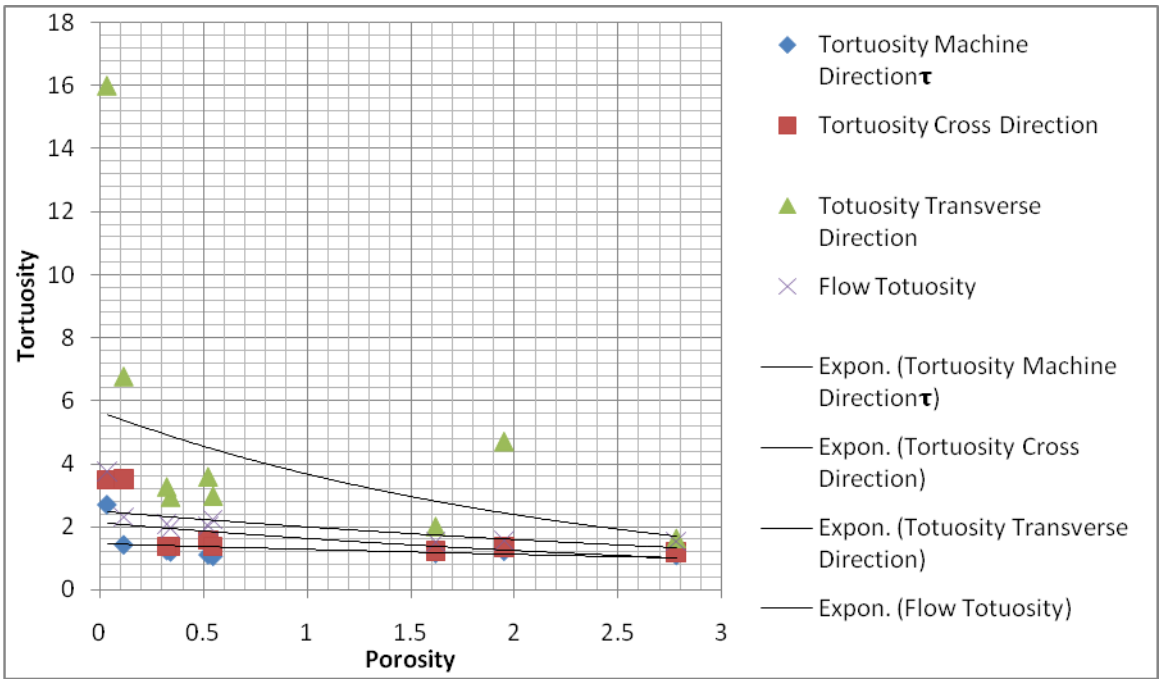

Figure-6

V. DISCUSSION AND RESULTS

The graphical representations with the help of table-3 are shown by the figure-6. The figure-6 shows that the toruosity varies inversely with porosity of the media. The tortuosities are given by the LB simulations and image analysis. The transverse and in plane tortuosities were determined by LB flow simulations and by image analysis that uses the chord length distribution algorithm [20]. The paper sheets formed as strictly layered structures in the laboratory sheet mold show little change in tortuosity with changing porosity as the fibres were refined the density of the sheet was increased. Hence, the transverse tortuosity has a significant change as a result of refining and densification. That indicates a more complex and less permeable structure. The chord length method tends to give higher values for tortuosity since the hydrodynamic tortuosity given by the LB method gives more weight to paths of least resistance, whereas this method does not prefer any particular fluid path or chord length.

REFERENCES

[1] Aaltosalmi U. Fluid flow in porous media with the Lattice-Boltzmann method, University of Jyväskylä, *Research report No*. 3/2005, Finland, *pp*.39-45.

[2] Antoine C., Nygard P., Gregersen Q. W., Weitkamp T., Rau C. 3D images of paper obtained by phase-contrast X-ray microtomography: image quality and binarisation, *Nucl. Inst. Meth. Phys. Res*. A 490 (2002), *pp*. 392–410.

[3] Aronsson M. On 3-D fibre measurements of digitized paper, Ph.D. thesis, *Swedish University of Agricultural Sciences* (2002).

[4] Bruschke M.V., Advani SG. Flow of generalized Newtonian fluids across a periodic array of cylinders. *J Rheol* 1993; 37(3) *pp*. 479–98.

[5] Chou T. Microstructural design of fiber composites. Cambridge: *Cambridge University Press*; 1992.

[6] Gebart B.R. Permeability of unidirectional reinforcements for RTM. *J Compos Mater* 1992; 26(8) *pp*.1100–1133.

[7] Goel A., Tzanakakis M., Huang S., Ramaswamy S., Choi D., Ramarao B. V. Characterization of the three-dimensional structure of paper using X-ray microtomography, *TAPPI J*. 84 (5) (2001), *pp*.1-8.

[8] Gooijer H, Warmoeskerken M.M.C.G., Wassink J.G. Flow resistance of textile materials – Part I: monofilament fabrics. *Text Res J*. 2003;73(5), *pp*. 437–443.

[9] Gureyev T. E., Evans R., Stevenson A. W., Gao D., Wilkins S. W. X-ray phasecontrast microscopy of paper, *TAPPI J*. 84 (2), (2001), *pp*. 52.

[10] Hu J. Structure and mechanics of woven fabrics. Cambridge: *Woodhead Publishing*; 2004.

[11] Huang S., Goel A., Ramaswamy S., Ramarao B. V., Choi D. Transverse and inplane pore structure characterisation of paper, *Appita J*. 55 (3) (2002), *pp*. 230-234.

[12] Lu W.M., Tung K.L., Hwang K.J. Fluid flow through basic weaves of monofilament filter cloth, *Text Res J*. 1996; 66(5), *pp*. 311–23.

[13] Markicevic B., Papathanasiou T,D. On the apparent permeability of regular arrays of non uniform fibers. *Phys. Fluids* 2002; 14(9), *pp*. 3347–3349.

[14] Nabovati A., Llewellin E.W., Sousa A. C. M. Through-thickness permeability prediction of three-dimensional multifilament woven fabrics, Composites: Part A, 41 (2010), *pp*. 453-463.

[15] Papathanasiou T.D. On the effective permeability of square arrays of permeable fiber tows. *Int J Multiph. Flow* 1997; 23(1), *pp*. 81–92.

[16] Papathanasiou T.D., Gravel E.M., Barwick S.C. Non-isotropic structured fibrous media: the permeability of arrays of fiber bundles of elliptical cross section, *Polym. Compos.* 2002; 23(4), *pp*. 520–529.

[16] Papathanasiou T.D. Flow across structured fiber bundles: a dimensionless correlation, *Int J Multiph. Flow* 2001; 27(8), *pp*.1451–1461.
[17] Pedersen G.C. Fluid flow through monofilament fabrics, *In: 64th national meeting of AIChE*, New Orleans; 1969.
[18] Pedersen G.C. Fluid flow through mono filament fabrics, *Filtr Sep*. 1974; 11(6), *pp*. 586–589.
[19] Ramaswamy S., Huang S., Goel A., Cooper A., Choi D., Bandyobadhyay A., Ramarao B. V. The 3D structure of paper and its relationship to moisture transport in liquid and vapor forms, in: The Science of Papermaking - trans.*12th Fundamental Research Symposium*, Vol. 2, The Pulp and Paper Fundamental Research Society, Bury, Lancashire, UK, 2001, *pp*. 1281–1311.
[20] Samuelsen E. J., Gregersen Q. W., Houen P. J., Helle T., Raven C., Snigirev A. Three-dimensional imaging of paper by use of synchrotron X-ray microtomography, *J. Pulp Pap. Sci*. 27 (2) (2001), *pp*. 50–53.
[21] Sangani A.S., Acrivos A. Slow flow past periodic arrays of cylinders with application to heat transfer, *Int. J. Multiph. Flow*, 1982; 8(3), *pp*.193–206.
[22] Sternberg S. R. Biomedical image processing, *IEEE Comp.*, 16 (1), (1983), *pp*. 22–34.
[23] Wang Q., Maze B., Tafreshi H.V. On the pressure drop modeling of monofilament-woven fabrics, *Chem. Eng. Sci*. 2007; 62(17), *pp*. 4817–4821.